International Journal of Concrete Structures and Materials
Vol.10, No.3, pp.383–391, September 2016
DOI 10.1007/s40069-016-0138-7
ISSN 1976-0485 / eISSN 2234-1315

Laboratory Simulation of Corrosion Damage in Reinforced Concrete

S. Altoubat[1),*], M. Maalej[1)], and F. U. A. Shaikh[2)]

(Received October 22, 2015, Accepted March 5, 2016, Published online March 17, 2016)

Abstract: This paper reports the results of an experimental program involving several small-scale columns which were constructed to simulate corrosion damage in the field using two accelerated corrosion techniques namely, constant voltage and constant current. A total of six columns were cast for this experiment. For one pair of regular RC columns, corrosion was accelerated using constant voltage and for another pair, corrosion was accelerated using constant current. The remaining pair of regular RC columns was used as control. In the experiment, all the columns were subjected to cyclic wetting and drying using sodium chloride (NaCl) solution. The currents were monitored on an hourly interval and cracks were visually checked throughout the test program. After the specimens had suffered sufficient percentage steel loss, all the columns including the control were tested to failure in compression. The test results generated show that accelerated corrosion using impressed constant current produces more corrosion damage than that using constant voltage. The results suggest that the constant current approach can be better used to simulate corrosion damage of reinforced concrete structures and to assess the effectiveness of various materials, repair strategies and admixtures to resist corrosion damage.

Keywords: corrosion, damage, potential, current, reinforced concrete.

1. Introduction

Chloride-induced steel corrosion is one of the major worldwide deterioration problems for steel reinforced concrete structures. Especially with the use of de-icing salts in cold climate regions, key bridge components such as the supporting columns are vulnerable to corrosion attack. Other sources of chloride contamination in structures may be saline contamination of aggregate component in concrete or the water used in concrete batching or from direct or indirect exposure to marine environments.

Much effort has been directed towards the design of new concrete mixes to reduce corrosion or establishment of sound techniques for the repair of existing structures (Bonacci and Maalej 2000). In order to evaluate the effectiveness of repair materials and methods in addressing reinforcement corrosion, accelerated corrosion techniques are often used.

Accelerated corrosion tests conducted in the laboratory are used to predict corrosion behaviour when service history is lacking and time or budget constraints prohibit field-testing (Davis 2000). While the desired service lives of many structures can range from 10 to 75 years, the typical time allowed for testing of candidate materials to support a materials selection process is measured in weeks or months. The purpose of any accelerated laboratory test is to provide reliable information on the performance of candidate materials or coatings in service. It is also typical that accelerated laboratory corrosion tests increase the severity of the environmental conditions, for example, by exposing the materials to more concentrated solutions, or increased periods of wetting. The environment used might simulate a humid tropical area, seaside air with high salt content, or one of many others.

Several research studies have used accelerated corrosion tests to study the corrosion resistance of reinforced concrete structural members incorporated new materials and/or designs. While several studies had employed a constant voltage accelerated corrosion regimes (Pellegrini-Cervantes et al. 2013; Deb and Pradhan 2013; Kishore Kumar et al. 2012; Lee et al. 2000; Al-Swaidani and Aliyan 2015), several others had also used constant current accelerated corrosion regimes (Talakokula et al. 2013; El Maaddawy et al. 2005; Kashani et al. 2013; El Maaddawy and Soudki 2003; Pritzl et al. 2014). One of the studies (El Maaddawy and Soudki 2003) focused on the effectiveness of the impressed (constant) current technique using current densities in the range of 100–500 μA/cm^2 to simulate corrosion of steel reinforcement in concrete. However, no studies could be found which had considered the effectiveness of the using constant voltage technique versus the constant current technique in simulating corrosion damage in reinforced concrete. In this paper, an experimental program is designed

[1)]Department of Civil & Environmental Engineering, College of Engineering, University of Sharjah, Sharjah, UAE.
*Corresponding Author; E-mail: saltoubat@sharjah.ac.ae
[2)]Department of Civil Engineering, Curtin University, Perth, Australia.

to study which of the two accelerated corrosion techniques (using constant voltage and constant current) produces more corrosion damage for similar amount of induced corrosion level (steel loss).

2. Research Significance

The success of any laboratory corrosion experiments depends largely on the ability of simulating field damage through an accelerated corrosion regime. In the field, significant corrosion damage is generated as a result of small percentage steel loss. In the laboratory, however, only minimal corrosion damage is generated as a result of high percentage steel loss. An ideal accelerated corrosion regime will not only produce the necessary damage within the required time frame, but produces damage that is consistent with that found in the field. This paper presents the evaluation of two different accelerated corrosion regimes: constant voltage and constant current to identify which of the two techniques provides a closer damage simulation to that in the field. As research work on corrosion is still being conducted to date using both techniques, the outcome of the present study will impact future research work in this field.

3. Test Program

3.1 Experimental Plan

The overall experimental program consists of two parts. The first part of the program is to allow test specimens to corrode to around 8 % steel loss using two methods of accelerated corrosion regimes, that is using constant voltage and constant current. The second part of the program is to structurally test the corroded specimens to failure by compression to determine the maximum compression load. The results will then be discussed in relation to the objectives of this study.

The test specimens used in this study were intended to simulate possible existing conditions in reinforced concrete bridge columns in which the concrete would be subjected to salt contamination. The test specimens were immersed in (3 % by weight of water) sodium chloride solution to simulate chloride contamination of the cover by the use of deicing salt spray. A total of six circular columns were constructed for this study.

3.2 Design of Specimen

The cross sectional details and overall dimensions of a typical column specimen are shown in Figs. 1 and 2, respectively. The largest possible dimension of the column specimen was selected such that it allows for ease of handling during the various stages of the experiment. Furthermore, the same column size was selected for all specimens in this comparative study. Incorporated into each column were six 13 mm diameter deformed reinforcing bars, oriented in the longitudinal direction of the column, and 6 mm diameter spiral at a spacing of 44 mm. A hollow stainless steel pipe with 20 mm diameter and 2 mm thickness was placed longitudinally in the centre of the column to act as a cathode. Holes of 2 mm in diameter were drilled on four sides at 20 mm spacing along the length of the hollow pipe within the test region to increase oxygen exposure. The reinforcing bars were also pre-drilled and tapped at the protruding end to facilitate the electrical connection from the power supply to the specimen.

To eliminate any possible end effects, the upper and lower 165 mm sections of the reinforcement cage were coated with epoxy to discourage corrosion.

3.3 Specimen Fabrication

Positioning of the six reinforcement bars and the centre cathode bar was done with the help of a wooden base, where bars were slotted in pre-drilled holes. The specimens were cast in the inverted position such that each bar protruded out of one end of the specimen by 15 mm when in the upright position. The protrusions of the bars were meant to allow connection of the electric circuit from the power supply to the specimens. After the main bars were put in place, spiral reinforcements were then tied to the main bars. Subsequently, epoxy coating was applied to both ends of the region of each specimen to prevent corrosion to these regions. Spacer blocks were also put along the spiral reinforcements to ensure required concrete cover. Large pipes of 208 mm diameter were also cut which formed the moulds of the specimens. A slit was made along the longitudinal direction of each pipe to facilitate the removal of the formwork upon demoulding. The slit was then closed by tying wires around the pipe. After that, the pipes were placed onto the wooden base and sealed along the circumference using silicone. Silicone was also applied along the slit to close up the gap.

One end of the stainless steel cathode bar which was going to be embedded in the concrete was taped to prevent concrete from flowing in during the pouring process. A plastic tubing of approximately the same diameter and length as the cathode bar was also inserted into the latter to prevent the cement and water from seeping through the numerous small holes drilled along the length of the cathode bar. The plastic tubing was meant to be removed after the concrete had hardened. Once that was done, the specimens were ready to be cast. After casting, the specimens were wrapped in plastic sheets and were subsequently cured outdoors using wet gunnysacks for 28 days.

3.4 Materials

Ordinary Portland cement was used for all concrete columns in this experimental program with 10 mm maximum coarse aggregate size. The concrete mix proportions for cubic meter of concrete is as follows: cement (OPC) = 300 kg; fine aggregate = 925 kg; coarse aggregate (10 mm) = 1000 kg, water = 185 kg, and admixture (Daracem 100) = 928 ml. The measured average 28-day concrete compressive cube strength was 29.02 MPa. The yield strengths of the 13 mm diameter round deformed bars and 6 mm diameter spiral reinforcing bars were 462 and 285 MPa, respectively.

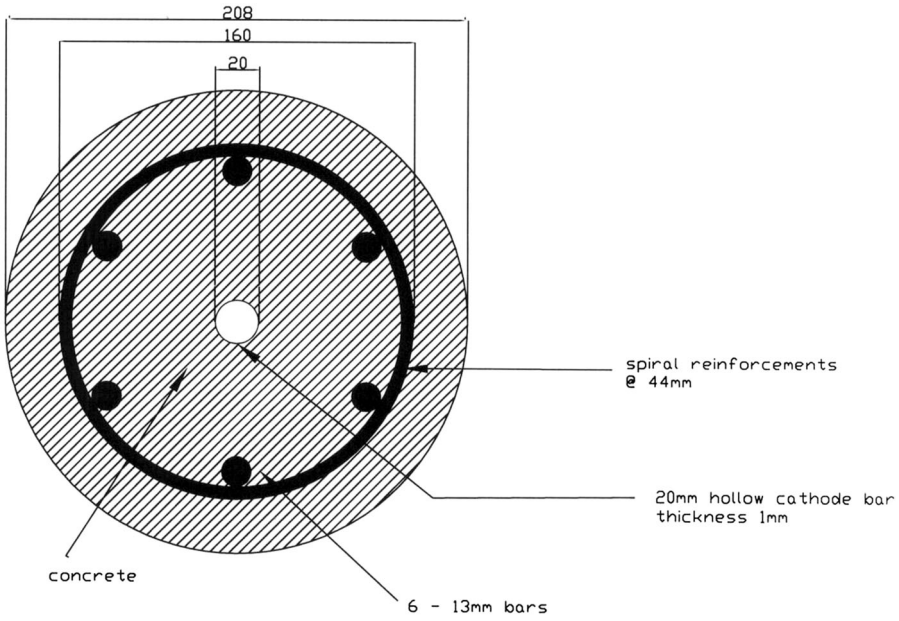

Fig. 1 Cross sectional details of the specimen.

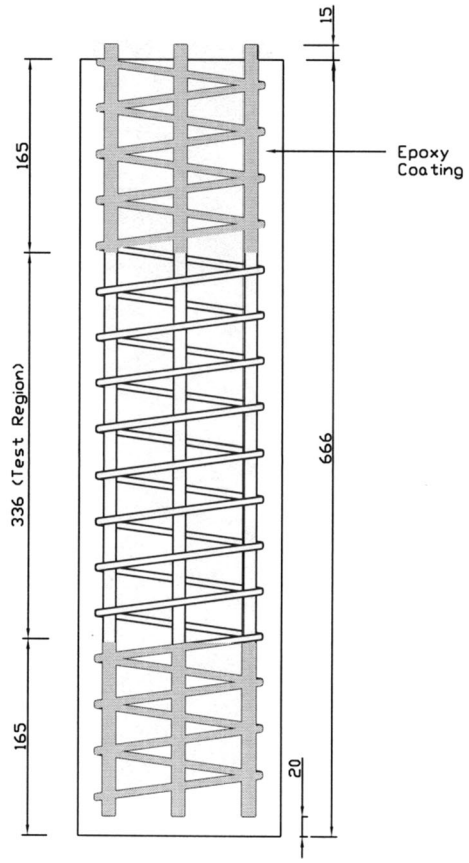

Fig. 2 Overall dimensions of a typical specimen.

3.5 Accelerated Corrosion Testing

Six concrete columns were tested in this study. Two out of the six concrete columns (labeled C1 and C2) were used as control for structural testing purpose and were not subjected to any accelerated corrosion. The remaining four columns were subjected to accelerated corrosion. Two concrete columns (labeled C3 and C4) were subjected to accelerated corrosion using constant voltage and two other concrete columns (labeled C5 and C6) were subjected to accelerated corrosion using constant current.

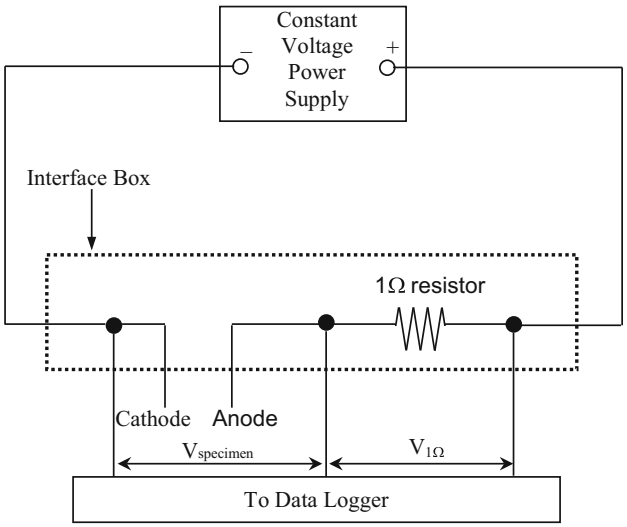

Fig. 3 Experimental setup for constant voltage.

All the columns (except the control) were subjected to cyclic wetting and drying using three percent sodium chloride (NaCl) solution by weight of water. The cycle is 1 day wet and two and a half days dry. During the wet cycle, the sodium chloride solution was filled up to the boundary of the upper test region and during the dry cycle, sodium chloride solution was pumped out to below the base level of the specimens. Matsuoka (1987) found that a cyclic wetting and drying test is more useful than continuous wetting or immersion in simulating actual field damage within a short time frame.

3.6 Constant Voltage Setup

Figure 3 shows a schematic diagram of the circuit setup for the accelerated corrosion test using constant voltage. The circuit basically consists of a one-ohm (1 Ω) resistor and the

specimen connected in series with the constant voltage power supply. The maximum voltage that the power supply can provide is 32 volts.

The 1 Ω resistor and the wires connecting the specimen to the circuit are contained in a specially designed interface box. Wires were also connected from the top of the interface box to the data logger to measure the output voltage readings across the specimen and the 1 Ω resistor.

3.7 Constant Current Setup

The experimental setup for accelerated corrosion under constant current is similar to that used for constant voltage except that the power supply is replaced by a constant current power supply.

3.8 Testing Procedure

First, the circuits for constant voltage and constant current were set up. Then, the circuits for the constant voltage were closed and the voltages across the 1 Ω resistor were recorded. According to Ohm's Law (V = IR), the current flowing in the circuit is effectively the same value as the voltage reading since the resistor has a resistance of 1 Ω. Next, the currents for the constant current circuits were adjusted such that at the start of the accelerated corrosion, all concrete columns were subjected to the same magnitude of corrosion current. The specimens were subsequently allowed to corrode and the current readings were taken on an hourly interval throughout the experiment until the desired percentage steel loss (i.e. 8 %) had been achieved. By knowing the voltage readings across the specimens, it was also possible to monitor the resistances of all the specimens throughout the experiment since the currents flowing in the various circuits were already known.

To accelerate the corrosion process, the specimens were subjected to cyclic wetting and drying. The cyclic wetting and drying will not only provide the necessary moisture for the corrosion reaction, but also a constant fresh supply of chloride ions to the reinforcement bars.

Pore saturation has two opposing effects (Liu and Weyers 1998): As pore saturation increases, the rate of corrosion increases too since the resistivity of the specimen decreases. However, the rate of oxygen diffusion, which is essential to corrosion, decreases. So initially, due to an improved conductivity, the corrosion rate will increase, but as time goes by, the corrosion rate decreases rapidly to a low value due to the strongly obstructed supply of oxygen. Therefore, to balance these opposing forces, it is important to find the optimum cycle which will be the most effective in producing corrosion damage in the specimens.

Based on a previous study by Lee et al. (2000), it was found that a cycle of 1 day wet and two and a half days dry produces the most corrosion damage to the specimens. So, in the present experiment, the 1 day (1 D) wet and two and a half days (2.5 D) dry cycle was adopted.

Throughout the experimental program, the corrosion current, circumferential expansion of the specimens and cracking were monitored on a periodic basis. From these, the amount of steel loss Δw calculated based on Faraday's Law using Eq. (1), extent of damage caused by the formation of expansive corrosion products and cracking pattern can be determined.

$$\Delta w = \frac{MIt}{zF} \tag{1}$$

where Δw = mass of steel consumed due to corrosion (grams), I is the current (amperes), t is the time (s), F is the 96,500 (amp s), z is the ionic charge (two for Fe), M is the atomic weight of metal (56 g for Fe).

It should be noted that other researchers have found that steel loss calculated using Faraday's Law tends to overestimate the actual steel loss (Aiello 1996). When the specimens are subjected to corrosion, the specimens will expand due to the formation of the corrosion products which are expansive in nature. To measure the circumferential expansion of each column, a specially fabricated mechanical expansion collar was placed at mid-height of each column. Each collar was made from 12 mm wide stainless steel sheets and included a small opening held closed by two stainless steel springs. A micrometer was used to measure the change in the opening size to the nearest one-hundredth of a millimeter, to determine the circumferential expansion of the column at mid-height.

After the concrete columns had achieved 8 % steel loss, the experiment was stopped and preparation works were done to the columns prior to structural testing. The protruding longitudinal reinforcement bars were cut off to level with the concrete surface.

In order for the columns to fail within the test region (since only the test region is allowed to corrode), both end regions of the columns were wrapped in glass fibre reinforced polymer wrap to strengthen the both ends.

All columns were tested under load control using an Instron Actuator IV testing machine with an ultimate capacity of 2000 kN to determine the maximum compression load. Two strain gauges were mounted horizontally along the circumference at the mid height of the test region, 180° apart to measure the circumferential strain. Located next to each horizontal strain gauge was another strain gauge mounted longitudinally to measure the longitudinal strain. In addition to that, two linear variable differential transducers (LVDT) were also placed 180° apart at the upper test region to measure the axial deformation. The gauge length of each LVDT was 50 mm. Figure 4 shows the setup prior to the start of the structural test.

4. Results and Discussion

4.1 Effect of Accelerated Steel Loss, Cracking and Circumferential Expansion

The following section presents the results obtained after around 48 days of accelerated corrosion for the four column specimens, excluding the controls, after the specimens had undergone sufficient corrosion. Steel loss, circumferential expansion and visual observation of cracking were used as

Fig. 4 Experimental setup for a typical column.

primary indicators of damage. The percentage steel losses at the end of the accelerated corrosion experiment for the constant voltage and constant current specimens were 8.13 and 8.10 %, respectively.

For the constant voltage specimens, an initial voltage of 12 volts was applied. The average output current reading was noted (0.5 A) and was subsequently applied to the constant current concrete specimens. However, after about 3 days of accelerated corrosion and upon computing the current densities, the applied constant voltage and applied contact current were reduced to 9.6 volts and 0.4 A, respectively to limit the current densities in the specimens to about 250 μA/cm^2. The currents passing through the four specimens undergoing accelerated corrosion over time are shown in Figs. 5 and 6.

The accumulated steel loss for the four specimens undergoing accelerated corrosion over time is shown in Fig. 7. Steel losses were calculated using Faraday's Law as indicated earlier. From the rate of steel loss over time plot shown in Fig. 8, it can be seen that the rate of steel losses for the constant current specimens are approximately constant throughout the experiment. However, for the constant

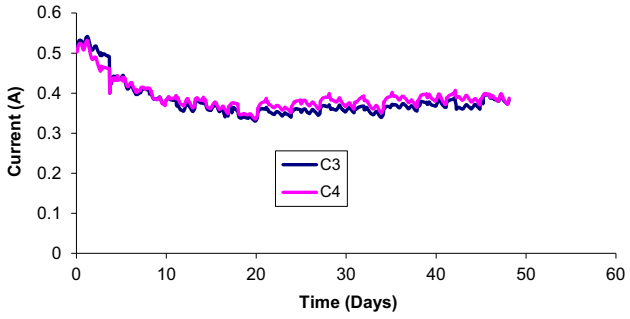

Fig. 5 Variation of current output with time for C3 and C4 (constant voltage).

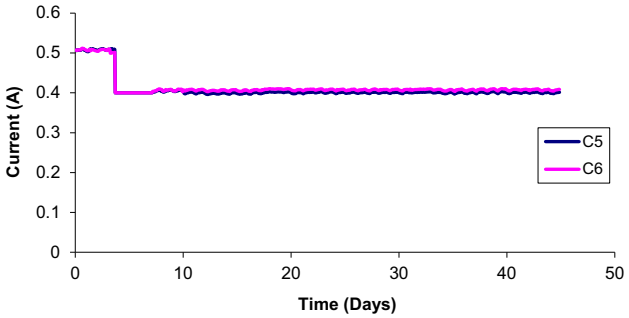

Fig. 6 Variation of current output with time for C5 and C6 (constant current).

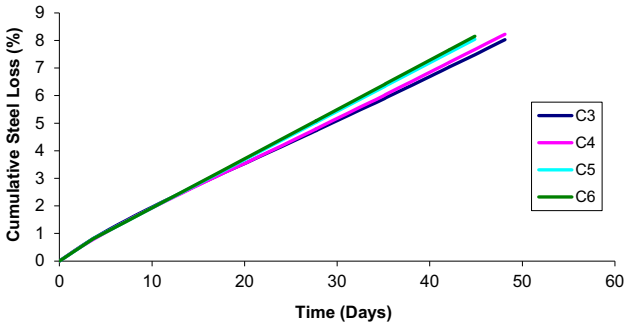

Fig. 7 Variation of cumulative steel loss with time for all specimens.

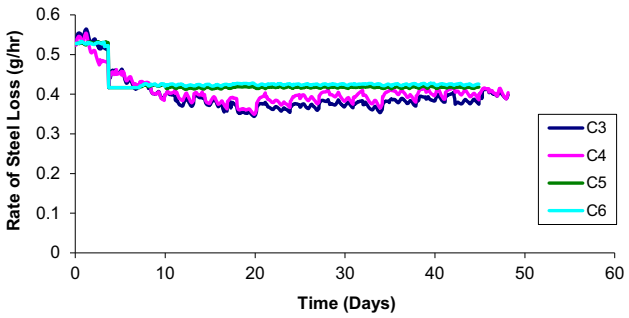

Fig. 8 Variation of the rate of steel loss with time for all specimens.

voltage specimens, there are fluctuations in the rate of steel losses. During the wet cycle, pore volumes get saturated, and the rate of corrosion increases as the resistivity of the specimen decreases. Consequently, more steel is being lost during the wet cycle which resulted in a peak in the rate of steel loss. Conversely, during the dry cycle, as water gets drained out, the pore volumes get less saturated and resistivity of the specimen increases, resulting in a lower current reading which is proportional to the rate of steel loss. Consequently, the steel loss during the dry cycles drops.

Circumferential expansion of each specimen undergoing accelerated corrosion was determined using a specially fabricated mechanical expansion collar fitted at mid height of the column. The circumferential strains at mid height for the various specimens over time are shown in Fig. 9. The graph shows that there was little circumferential expansion for the first 14 days. Subsequently, the constant current specimens (C5 and C6) began to show significant increases

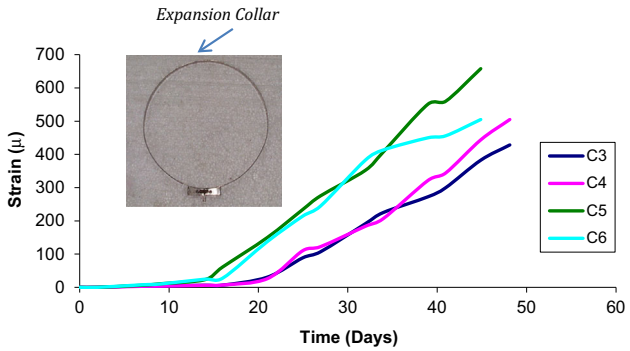

Fig. 9 Variation of the circumferential expansion with time for all specimens as measured with mechanical expansion collar.

in the circumferential strain. The constant voltage specimens (C3 and C4) took around 21 days for significant circumferential expansion to take place. At any given time beyond the first 14 days, the expansion was more for the constant current specimens than for the constant voltage specimens as seen in Fig. 9. Since, circumferential expansion is one of the primary indicators of damage, it can be said that the constant current specimens suffered more damage than constant voltage specimens, although the percentage steel losses were comparable (8.10 % for constant current versus 8.13 % for constant voltage).

The specimens were constantly checked for any visual cracks on the surfaces, especially within the test regions. For both constant current concrete specimens C5 and C6, visible cracks were observed after approximately 15 days of accelerated corrosion. But for the constant voltage specimens, no visible cracks were observed until after approximately 19 days.

For all specimens, cracking began initially as short, vertical and discontinuous in the longitudinal direction near the upper test region. However, as time went by, the cracks began to propagate longitudinally in both directions and some of the vertical cracks joined together. Existing cracks were also seen to be widening. The number and location of each crack was sketched, approximately to scale, on paper as they appeared on the specimen. Typical crack patterns are shown in Figs. 10, 11, for the constant voltage and constant current specimens, respectively.

Horizontal cracks were also observed at the upper test region for both constant current concrete specimens towards

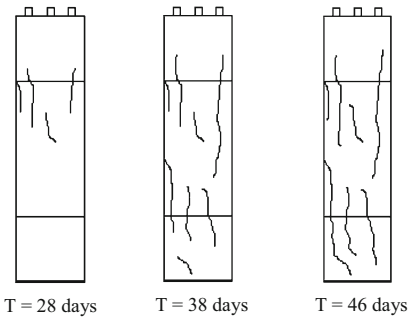

Fig. 10 Typical cracking patterns for constant voltage specimens (C3 in this figure).

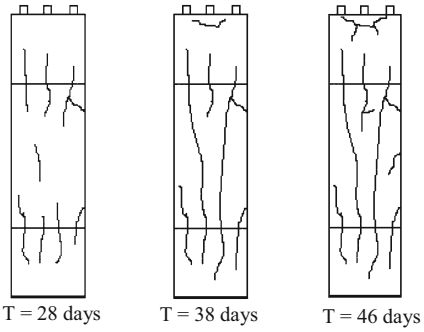

Fig. 11 Typical cracking patterns for constant current specimens (C5 in this figure).

the end of the experiment. However, this was not observed in the constant voltage specimens. Also, there were signs of delamination at the top concrete face where the reinforcement bars protruded for electrical connection for both constant current specimens.

From the observation of cracking patterns of the concrete specimens, it is clear that there were more cracks that had formed in the constant current specimens than in the constant voltage specimens. The cracks observed in the constant current specimens were also longer and the maximum crack widths measured were also larger than those in the constant voltage specimens as shown in Table 1. Photos of developed cracks at the end of the accelerated corrosion regimes are shown in Fig. 12.

One observation from the result is that, in Fig. 8, the general trend lines for the constant voltage specimens are such that the rate of steel loss decreased to a certain value (at around 20 days after the start of the experiment) and subsequently, started to slowly increase. This increase in the rate of steel loss can be explained by the marked increase in the circumference expansion in the specimens themselves. It was observed that the time for significant circumferential expansion of both constant voltage specimens to occur (as shown in Fig. 9) was around 21 days, which was quite close to the time when the steel loss increased. That coincided with the time when first visual cracking of the specimens was being observed (i.e. at 19 days). This means that, the first appearance of the cracks provided easier access for the chloride ions to reach the steel bars and attack them. As more chloride ions made their way to the steel bars through the cracks, the steel bars were more vulnerable to corrosion attack than before and consequently, the steel loss was increased.

4.2 Effect of Accelerated Corrosion on Structural Response

Structural testing was performed on all the specimens (including the control specimens) after wrapping both ends of each column with GFRP sheets to determine the maximum compression load. After all the specimens C1 to C6 had undergone structural testing, the results were compiled and analyzed. Upon preliminary analysis of the results, it was decided that the results for both specimens C1 (control) and C6 (constant current) to be disregarded. The basis for

Table 1 Test summary results of C2, C3, C4 and C5 and maximum crack width for columns C3 to C6.

Specimen	Steel loss percentage	Maximum load (kN)	Strength reduction (%)[#]	Corresponding axial deformation (mm)	Max crack width (mm)
C2 (control)	–	1100	–	3.8	–
C3 (constant voltage)	8.02	1043	5.2	1.4	0.38
C4 (constant voltage)	8.23	1045	5.0	1.6	0.42
C5 (constant current)	8.04	996	9.5	1.0	0.54
C6 (constant current)	8.15	–	–	–	0.46

[#] Strength reductions were calculated with reference to the control specimen.

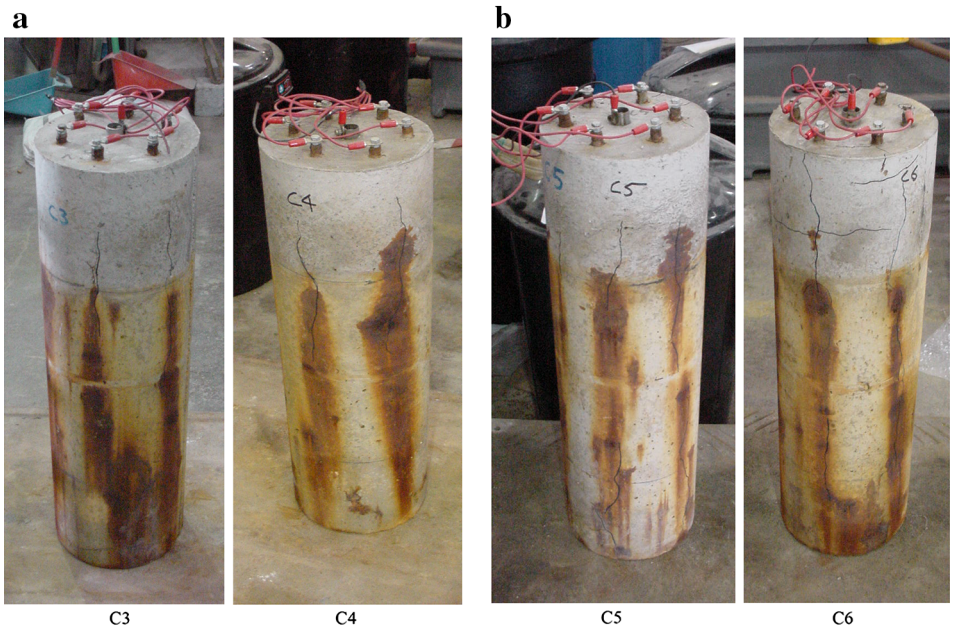

Fig. 12 **a** Cracking at the end of constant voltage corrosion process. **b** Cracking at the end of constant current corrosion process.

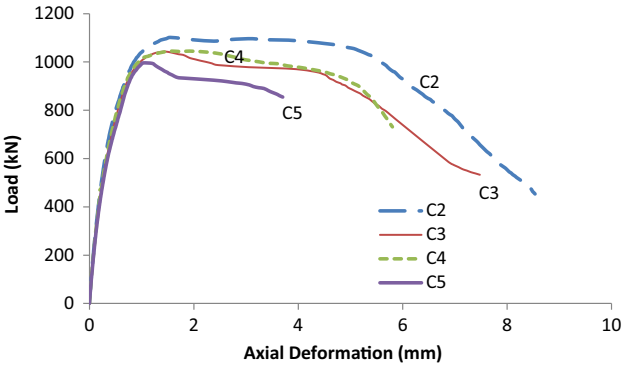

Fig. 13 Plots of axial load versus axial deformation for all column specimens.

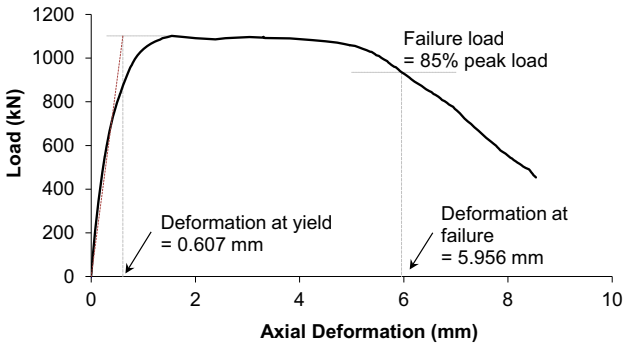

Fig. 14 Axial load versus axial deformation curve for specimen C2.

disregarding the results for these specimens was that the loadings for both specimens were not concentric. From the structural test data, the reduction in compression load for both the constant current and constant voltage specimens was compared. Since the amount of steel loss in both types of specimens were approximately the same, the group of specimens that yielded higher reduction in maximum compression load would be the ones that suffered greater corrosion damage.

A summary of the structural test results is also shown in Table 1 for comparison purpose. From this table, it is clear that the reduction in the maximum compression load for the constant current specimen is more than those for the constant voltage specimens. The performances of the constant current and constant voltage specimens were also compared with that of the control in the superimposed plot shown in Fig. 13. Since the concrete specimens which had undergone accelerated corrosion experienced similar percentage steel

Table 2 Ductility ratios for specimens C2, C3, C4 and C5.

Specimen	Axial deformation (mm)		Ductility ratio
	At yield	At failure	
C2 (control)	0.607	5.956	9.81
C3 (constant voltage)	0.61	5.019	8.23
C4 (constant voltage)	0.61	5.218	8.55
C5 (constant current)	0.61	3.790	6.21

loss of approximately 8 %, it can be concluded that the constant current specimen (with 9.5 % strength reduction) experienced greater strength reduction per percentage steel loss than constant voltage specimens (with an average of 5.1 % strength reduction).

The performances of the concrete columns (including the control) were also evaluated in terms of ductility. The parameter used in the evaluation was the ductility ratio which is defined as the ratio of deformation at failure to the deformation at yield. It was calculated based on a previous study containing similar analysis (Sheikh et al. 1997). The higher the ductility ratio, the more ductile is the specimen.

To find out the deformation at yield, a straight line, which passed through the point of peak load, was drawn parallel to the minor axis as shown in Fig. 14. Next, another straight line was drawn from the origin, joining the point on the load-deformation curve corresponding to 65 % of the peak load. This line was then extrapolated to intersect the earlier line. The corresponding deformation at the point of intersection was taken as the deformation at yield. Failure load was taken to be 85 % of the peak load. The deformation at failure was obtained directly from the point corresponding to 85 % of the peak load from the graph. Table 2 shows the results of the ductility ratios for specimens C2, C3, C4, and C5.

From the calculated values of the ductility ratios, it can be seen that the corroded specimens with constant current suffered a loss of ductility when compared to the control specimen. This is indicative of greater corrosion damage in the constant current specimen.

5. Conclusions

Six small-scale circular columns were cast for the purpose of comparing two types of accelerated corrosion techniques, namely constant voltage and constant current. The result of this study can be summarized as follows:

1. With respect to corrosion damage, it was observed that during the corrosion process, there were more longitudinal cracks in the constant current specimens than in the constant voltage specimens. Also, the maximum crack widths for the constant current specimens were greater than those of the constant voltage specimens. Furthermore, the constant current specimens also experienced greater circumferential expansion than the constant voltage specimens. Considering all of these visual indicators of damage, and considering that both methods produced similar steel loss, it can be said that the constant current specimens showed greater signs of damage than the constant voltage specimens. Hence, it can be concluded that accelerated corrosion using constant current is recommended over the constant voltage in studying the effectiveness of various materials, repair strategies and admixtures to resist corrosion damage.
2. With respect to structural response, it was found that there was a greater reduction in the load carrying capacity of the constant current specimen than in the constant voltage specimens when compared to that of the control. In addition, the constant current specimen behaved in a less ductile manner than the constant voltage specimens. Therefore, it can be concluded that accelerated corrosion using constant current also produces greater structural damage to the concrete columns than using constant potential.

In light of the above results, and when considering the use of electro-chemical methods to simulate corrosion in reinforced concrete, it would be recommended to employ a constant current technique rather than a constant voltage technique. In terms of target corrosion current, earlier Laboratory tests had shown that the use of current densities in the range of 100–500 $\mu m/cm^2$, produces theoretical mass losses of the steel reinforcement (based on Faraday's Law) that are in good agreement with measured mass losses based on gravimetric weight loss measurement procedures.

Acknowledgments

Support for this research was provided in part by the Sustainable Construction Materials and Structural Systems (SCMASS) research group at the University of Sharjah. This support is gratefully acknowledged.

Open Access

References

Aiello, J. (1996). The effect of mechanical restraint and mix design on the rate of corrosion in concrete. MEng. Thesis, Department of Civil Engineering, University of Toronto, Toronto, Canada.

Al-Swaidani, A. M., & Aliyan, S. D. (2015). Effect of adding scoria as cement replacement on durability-related properties. *International Journal of Concrete Structures and Materials, 9*(2), 241–254.

Bonacci, J. F., & Maalej, M. (2000). Externally-bonded FRP for service-life extension of RC infrastructure. *ASCE Journal of Infrastructure Systems, 6*(1), 41–51.

Davis, J. R. (2000). *Corrosion: Understanding the basics, materials park*. Novelty, OH: ASM International.

Deb, S., & Pradhan, B. (2013). A study on corrosion performance of steel in concrete under accelerated condition. In Proceedings of the International Conference on Structural Engineering Construction and Management, Kandy, Sri Lanka, December 13th–15th 2013.

El Maaddawy, T. A., & Soudki, K. A. (2003). Effectiveness of impressed current technique to simulate corrosion of steel reinforcement in concrete. *Journal of Materials in Civil Engineering, 15*(1), 41–47.

El Maaddawy, T. A., Soudki, K. A., & Topper, T. (2005). Analytical model to predict nonlinear flexural behavior of corroded reinforced concrete beams. *ACI Structural Journal, 102*(4), 550–559.

Kashani, M. M., Crewe, A. J., & Alexander, N. A. (2013). Nonlinear stress–strain behaviour of corrosion-damaged reinforcing bars including inelastic buckling. *Engineering Structures, 48*, 417–429.

Kumar, M. K., Rao, P. S., Swamy, B. L. P., & Mouli, C. C. (2012). Corrosion resistance performance of fly ash blended cement concretes. *International Journal of Research in Engineering and Technology, 1*(3), 448–454.

Lee, C., Bonacci, J. F., Thomas, M. D. A., Maalej, M., Khajehpour, S., Hearn, N., Pantazopoulou, S., & Sheikh, S. (2000). Accelerated corrosion and repair of reinforced concrete columns using CFRP sheets. *Canadian Journal of Civil Engineering, 27*(5), 941–948.

Liu, T., & Weyers, R. W. (1998). Modeling the dynamic corrosion process in chloride contaminated concrete structures. *Cement and Concrete Research, 28*(3), 365–379.

Matsuoka, K. (1987). Monitoring of corrosion of reinforcing bar in concrete. In CORROSION/87 Symposium on Corrosion of Metals in Concrete. Houston, TX: National Association of Corrosion Engineers.

Pellegrini-Cervantes, M. J., et al. (2013). Corrosion resistance, porosity and strength of blended portland cement mortar containing rice husk ash and nano-SiO_2. *International Journal of Electrochemical Science, 8*, 10697–10710.

Pritzl, M. D., Tabatabai, H., & Ghorbanpoor, A. (2014). Laboratory evaluation of select methods of corrosion prevention in reinforced concrete bridges. *International Journal of Concrete Structures and Materials, 8*(3), 201–212.

Sheikh, S., Pantazopolou, S., Bonacci, J. F., Thomas, M. D. A., & Hearn, N. (1997). Repair of delaminated circular pier columns by ACM. Ontario Joint Transportation Research Report, Ministry of Transportation Ontario (MTO).

Talakokula, V., Bhalla, S., & Gupta, A. (2013). Corrosion assessment of reinforced concrete structures based on equivalent structural parameters using electro-mechanical impedance technique. *Journal of Intelligent Material Systems and Structures*. doi:10.1177/1045389X13498317.